

SING: A Plug-and-Play DNN Training Technique

Adrien Courtois¹ Damien Scieur² Jean-Michel Morel¹ Pablo Arias^{1,*} Thomas Eboli^{1,*}

¹ Université Paris-Saclay, ENS Paris-Saclay, Centre Borelli, France ² Samsung SAIL, Canada

Abstract

We propose SING (Stabilized and Normalized Gradient), a plug-and-play technique that improves the stability and generalization of the Adam(W) optimizer. SING is straightforward to implement and has minimal computational overhead, requiring only a layer-wise standardization of the gradients fed to Adam(W) without introducing additional hyper-parameters. We support the effectiveness and practicality of the proposed approach by showing improved results on a wide range of architectures, problems (such as image classification, depth estimation, and natural language processing), and in combination with other optimizers. We provide a theoretical analysis of the convergence of the method, and we show that by virtue of the standardization, SING can escape local minima narrower than a threshold that is inversely proportional to the network’s depth.¹

1 Introduction

Neural network training is a highly non-convex and stochastic optimization problem, complicated by hidden dynamics between the optimization algorithm and the network architecture. Several common pitfalls have been identified, such as bad initialization, vanishing and exploding gradients [3, 34], abrupt shifts in the distribution of layer inputs (the so-called internal covariate shift [21]). Significant progress has been made by tackling these issues either by architectural improvements [1, 19] or with better optimizers [23, 30, 41].

The Adam(W) optimizer [23, 28] is widely adopted for neural network training due to its ability to combine first and second-order moments of the gradient, mitigating the sensitivity to the learning rate, and providing adaptability to gradient updates of different magnitude or sparsity. It is applicable to widely different architectures, from convolutional to transformers, and application domains. Nonetheless, it has shown instabilities in specific scenarios, such as large-scale problems [6, 31] or, as we demonstrate in this work, some image-to-image tasks. These instabilities manifest as spikes in the training loss which might involve a prolonged recovery periods - if it recovers.

Contributions. In this work we propose a simple layer-wise gradient standardization as a technique to improve the stability of existing optimizers. Our technique, SING, is plug-and-play: by simply changing the gradient fed to AdamW (or any other “host” optimizer) it integrates seamlessly without introducing any additional hyperparameters. As such, it does not require any additional fine-tuning apart from that of the host optimization framework. In this way, SING preserves the desirable properties of the host optimizer but with increased stability.

We notably theoretically show that the optimizer is capable to escape narrow local minima *within a single step*, given a sufficiently high learning rate (see Theorem 3.1). Moreover, the magnitude of this learning rate is *inversely proportional* to the depth of the network *i.e.* for a fixed learning rate, the higher the number of layers of the network, the lower the learning rate must be to escape local

*Equal supervision.

¹The code is available at <https://github.com/AdrienCourtois/SING>.

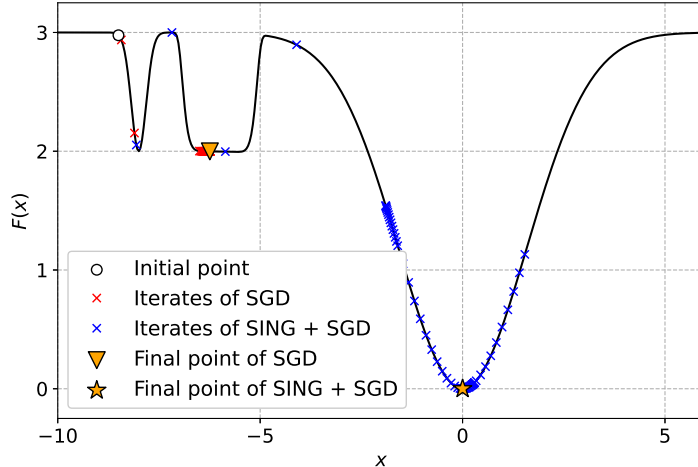


Figure 1: Optimization of a function with three local minima. A gradient descent (noted SGD) with the proposed gradient standardization SING can escape narrow local minima (Theorem 3.1). SING steps jump over narrow local minima in one step. Conversely, SGD without SING steps jump over the first local minimum but stays blocked in the second one because the gradient amplitude is too small. The learning rate is reduced using a cosine decay.

minima. This highlights the compatibility of our technique with deep neural networks. Since narrow local minima are often associated with poor generalization in non-convex optimization landscapes [7, 17, 18, 22, 35], it is crucial for an optimizer to avoid such pitfalls. We capitalize on this theoretical result and stabilize the gradient using several techniques [20, 42, 60] to reach a step size as large as possible, and thus escape from as many local minima as possible.

Although our initial focus was to address Adam’s limitations, our technique demonstrates robust generalization even in tasks where Adam performs well. Notably, we show improvements over AdamW on several tasks such as image classification, depth estimation and natural language processing.

The paper is organized as follows. Section 2 describes the proposed method, followed by its theoretical analysis in Section 3 where the properties of SING are presented. We discuss related work in Section 4. In Section 5 we provide extensive numerical experiments which demonstrate the effectiveness of the proposed method on a variety of tasks in natural language processing and computer vision.

2 Algorithm

We seek to approximate the solution to the following optimization problem,

$$\min_{x \in \mathbb{R}^p} F(x). \quad (1)$$

We assume there exists a random function $f : \mathbb{R}^p \rightarrow \mathbb{R}$ such that $\mathbb{E}[\nabla f(x)] = \nabla F(x)$ for all $x \in \mathbb{R}^p$, and that we have access to an oracle providing i.i.d. samples $(f_n)_{n \in \mathbb{N}}$ [10].

In the case of neural networks, the optimization variable x represents the parameters of the network, F is the oracle loss and f is the empirical loss evaluated on a random mini-batch. The parameters of a neural network have a specific structure. They are made of the concatenation of the parameter tensors from each layer of the network. We use $D \in \mathbb{N}$ to denote the number of these parameters tensors and define $(I_k)_{k \in \llbracket 1, D \rrbracket}$ such that $x_{I_k} = \{x_i : i \in I_k\}$ represents the k -th parameter tensor. As an example, let’s consider the neural network $\mathcal{N}(\cdot; A, b) = A \cdot + b$. In this case, the network has two parameter tensors, hence $D = 2$. The first parameter tensor is $x_{I_1} = A$ and the second is $x_{I_2} = b$.

Our objective is to endow an optimizer with several key properties: **1)** stability **2)** capacity to escape narrow local minima **3)** adaptability to geometry of the energy landscape, and **4)** convergence. Importantly, we want to achieve all of these properties without adding any additional hyper-parameters and with minimal computational overhead. We achieve the first property – stability – by dividing the gradient by its norm. This prevents vanishing and exploding gradients, which can lead to unstable


```

def optim_step(model, lr, beta, weight_decay,  $\epsilon$ ):
    for p in model.parameters():
        # Standardization
        p.grad = centralize(p.grad)
        p.grad = normalize(p.grad,  $\epsilon$ )
        # Weight decay
        p = p * (1 - lr * weight_decay)
        # Optimizer
        update = optimizer(p.grad, beta)
        # Parameter update
        p = p - lr * update

def centralize(grad):
    if grad.dim() > 1:
        dims = tuple(range(1, grad.dim()))
        mean = grad.mean(dims, keepdim=True)
        grad = grad - mean
    return grad

def normalize(grad,  $\epsilon$ ):
    grad = grad / (grad.norm() +  $\epsilon$ )
    return grad

```

Algorithm 2: PYTORCH implementation of our algorithm. The Γ operator is implemented by NORMALIZE and ϕ by CENTRALIZE. Our technique can be used within any existing first order method *i.e.* the OPTIMIZER function can be any optimizer (see Table 3 for a comparison).

training. This also allows to use fixed gradient steps, which enables the algorithm to move past narrow local minima, as we show in the next section.

We define the steps taken by our optimizer by

$$x_{t+1} = x_t - \eta \frac{\phi(\nabla f(x_t))}{\Gamma(\phi(\nabla f(x_t)))}, \quad (2)$$

where ϕ is the gradient centralization operation [51] and the division is applied element-wise. The operator Γ corresponds to the parameter-wise normalization *i.e.*

$$\Gamma(x)_i = \|x_{I_k}\|_2, \quad \text{where } k \in \llbracket 1, D \rrbracket \text{ and } i \in I_k. \quad (3)$$

In theory, there could be a division by zero in (2). To avoid this we can add $\epsilon = 10^{-8}$ to the denominator although it is not strictly necessary because the gradient norm is large in practice. This parameterization naturally arises in usual Deep Learning frameworks, see Algorithm 2 for the PYTORCH implementation.

Our setting differs from regular normalized gradient descent in two ways: we center the gradients before normalizing and we perform the normalization on a parameter-wise basis. This is particularly important for large networks where the norm of the full gradient can be very large, making it nearly impossible to train the network effectively.

3 Theoretical Analysis

This section analyzes the key properties of our technique. Theorem 3.1 demonstrates how normalization techniques aid in escaping local minima. Theorem 3.2 establishes stability results, including several invariance properties of the algorithm. Moreover, Theorems 3.3 and 3.4 provide insights into the rate of convergence of our algorithm in a stochastic setting, under mild assumptions. For complete proofs and technical details, please refer to Appendix A.

3.1 Escaping from narrow local minima

One of the key properties of our algorithm is its ability to escape from narrow local minima. This is crucial because the stochasticity of the optimization landscape often leads to the creation of artificial local minima, generally associated with poor generalization performance [7, 17, 18, 22, 35]. To achieve this we normalize the gradient to take fixed-size steps during training, where the learning rate controls the step size. Doing so allows the escape from narrow local minima provided the steps are large enough. This property is central to our algorithm and leads to better generalization performance.

For simplicity, we assume a deterministic setting in this section. We show that the normalization procedure helps the optimizer to escape narrow local minima. To formalize this observation, we first define the *basin of attraction* of a critical point of F .

Definition 3.1. Let x^* be a critical point of F . The basin of attraction of x^* is defined to be the set $W(x^*)$ such that

$$W(x^*) \stackrel{\text{def}}{=} \{x \in \mathbb{R}^p : \langle \nabla F(x), x - x^* \rangle \geq 0\}.$$

Moreover, we write $\mathcal{B}(x^*)$ to be the largest ball contained within $W(x^*)$, and r its radius.

In the previous definition, if x^* is a saddle point, $A(x^*) = \{x^*\}$ and $r = 0$.

Theorem 3.1 (Escaping from narrow local minima). Let x_t be the sequence of iterates defined by (2) and y_t the sequence of iterates of gradient descent,

$$y_{t+1} = y_t - \eta_{\text{GD}} \nabla F(y_t). \quad (4)$$

Assume that $x_t \in \mathcal{B}(x^*)$ (resp. $y_t \in \mathcal{B}(x^*)$) i.e. the ball contained in the basin of attraction of x^* , defined in Definition 3.1. Also, assume that x_t (resp. y_t) is not a critical point i.e. $\nabla F(x_t) \neq 0$ (resp. $\nabla F(y_t) \neq 0$). If the stepsize is sufficiently large,

$$\eta_{\text{SING}} \geq \frac{2r}{\sqrt{D}}, \quad \eta_{\text{GD}} \geq \frac{2r}{\|\nabla F(y_t)\|_2}, \quad (5)$$

then the iterates x_{t+1} (resp. y_{t+1}) is outside the set $\mathcal{B}(x^*)$. See Figure 1 for an illustration.

We see that GD struggles to escape local minima: under mild assumptions on ∇F , the closer y_t is to x^* the higher the learning rate must be to escape from $A(x^*)$. Indeed, for GD there is no finite step-size η_{GD} that guarantees escaping $A(x^*)$. In contrast, Theorem 3.1 tells us that our algorithm escapes $A(x^*)$ in a single step, provided the learning rate is sufficiently large. Furthermore, as the number of parameter tensors in the model increases, it becomes easier to escape from $A(x^*)$. This is an important advantage of our algorithm over GD, especially for large models where the optimization landscape can be highly complex and difficult to navigate.

When the Hessian at x^* is well conditioned, escaping from $A(x^*)$ is roughly equivalent to escaping from the local minimum. Therefore, it is crucial to use the highest possible learning rate. However, using a high learning rate can be problematic as the gradients are unstable and tend to oscillate leading to suboptimal convergence. To address this issue, several methods have been proposed to stabilize the gradients and allow for larger learning rates. Such methods include gradient centralization, LookAhead [57], different momentum strategies such as Adam [23], AdaBelief [60] or even AdaFactor [39] and larger batch sizes, among others. For this reason, the final implementation of our algorithm incorporated within AdamW features LookAhead and softplus calibration [42]. Note however that it does not introduce any additional hyper-parameters as the parameters of these stabilization methods are fixed once and for all.

3.2 Invariance properties

In this section, the setting is considered deterministic for simplicity. This section examines the invariance properties of the technique.

Firstly, we show that a rescaling of the objective function,

$$\min_{x \in \mathbb{R}^p} \tilde{F}(x) \stackrel{\text{def}}{=} \alpha F(x), \quad \alpha > 0. \quad (6)$$

does not affect the updates. This property is desirable as the network’s performance is unaffected by a scaling of the loss. A similar invariance property applies to changes during training that cause a rescaling of the gradients of a layer. If during training, the output of one layer of the network is rescaled, it won’t affect the update of the previous layers, thus alleviating part of the problem of internal covariate shift [21].

Second, the algorithm presented in this paper preserves the mean i.e.

$$\sum_{i=1}^p [x_{t+1}]_i = \sum_{i=1}^p [x_t]_i, \quad (7)$$

where $[x]_i$ corresponds to the i -th component of the vector x .

Theorem 3.2. The iterates defined by (2) are invariant w.r.t. transformation (6), and preserve the mean (7).

The property of preserving the mean has been demonstrated to improve the stability of the optimization process in deep neural networks [51]. Moreover, it is motivated by the observation that many non-linear layers demonstrate a mean-shift behavior [21], which alters their behavior based on the sign of input values. This mean-shift behavior is mitigated by the presence of normalization layers, that re-scale and shift the weights. Preserving the mean enhances the stability of the optimization dynamics when normalization layers are present.

Furthermore, normalizing the centered gradients mitigates a potential pathological scenario where the gradient signal is diminished. Indeed, the mean of the gradient can hinder the important signal when the mean is too large compared to the centered gradient [51]. However, in such case the amplitude of the centered gradient can be relatively small, preventing efficient updates. Normalizing the gradient solves this issue by preserving its amplitude.

3.3 Convergence

In this section, two theorems of convergence are provided. In the first one, the normalization is studied without the centralization. Under mild assumptions, we show the ℓ^2 -norm of the gradient can be reduced to any desired precision. In the second one, we consider the full setting and show the same result for the ϕ -norm (which is a pseudo-norm). We assume that the stochastic gradient has a σ -bounded variance ($\sigma > 0$) *i.e.*

$$\forall x \in \mathbb{R}^p, \mathbb{E} [\|\nabla F(x) - \nabla f(x)\|_2^2] \leq \sigma^2, \quad (8)$$

and the objective function F is positive and L -smooth,

$$\forall x, y \in \mathbb{R}^d, \|\nabla F(x) - \nabla F(y)\|_2 \leq L\|x - y\|_2. \quad (9)$$

Theorem 3.3 (Convergence without gradient centralization). Let assumptions (8) and (9) hold. Assume the gradient is computed across a mini-batch of size $B = \frac{\sigma^2}{\epsilon^2}$. Let x_t be the sequence of iterates (2) with $\phi = I$. Then, we have

$$\frac{1}{T} \sum_{t=0}^{T-1} \mathbb{E}[\|\nabla F(x_t)\|_2] \leq \frac{F(x_0)}{\eta T} + (1 + \sqrt{D})\epsilon + \frac{\eta LD}{2}. \quad (10)$$

If we set $\tau \sim \mathcal{U}([0, T-1])$, $\eta = \frac{2\epsilon}{L}$ and $T = \frac{LF(x_0)}{2\epsilon^2}$, we obtain $\mathbb{E}[\|\nabla F(x_\tau)\|_2] \leq (2 + \sqrt{D} + D)\epsilon$. Therefore, the iteration complexity and computation complexity to achieve an ϵ -stationary point are $\mathcal{O}(1/\epsilon^2)$ and $\mathcal{O}(1/\epsilon^4)$, respectively.

Theorem 3.4 (Convergence with gradient centralization). Let assumptions (8) and (9) hold. Assume the gradient is computed across a mini-batch of size $B = \frac{\sigma^2}{\epsilon^2}$. Let x_t be the sequence of iterates (2). Then we have

$$\frac{1}{T} \sum_{t=0}^{T-1} \mathbb{E}[\|\nabla F(x_t)\|_\phi] \leq \frac{F(x_0)}{\eta T} + (1 + \sqrt{D})\epsilon + \frac{\eta LD}{2}, \quad (11)$$

where $\|\cdot\|_\phi^2 = \langle \cdot, \phi(\cdot) \rangle_2$ is a pseudo-norm. If we set $\tau \sim \mathcal{U}([0, T-1])$, $\eta = \frac{2\epsilon}{L}$ and $T = \frac{LF(x_0)}{2\epsilon^2}$, we obtain $\mathbb{E}[\|\nabla F(x_\tau)\|_\phi] \leq (2 + \sqrt{D} + D)\epsilon$. Therefore, the iteration complexity and computation complexity to achieve an (ϵ, ϕ) -stationary point are $\mathcal{O}(1/\epsilon^2)$ and $\mathcal{O}(1/\epsilon^4)$, respectively.

Note that Theorem 3.4 only gives us an (ϵ, ϕ) -stationary point *i.e.* in the limit $\epsilon \rightarrow 0$, $\nabla F(x_\tau)$ converges to a point in $\text{Ker}(\phi) = \text{Span}((1, \dots, 1)^T)$. Indeed, applying ϕ to the gradients amounts to do a projected gradient descent onto the set of weights with the same mean as the initial weights.

We argue that this “weaker” convergence result it is not problematic. Reaching a point in $\text{Ker}(\phi)$ means that the optimization process cannot go any further without violating the constraint. However, since neural networks have lots of parameters, adding one constraint to the solution is not likely to lead to worse performance [51].

4 Related Work

The most-used optimizer nowadays is Adam [23], which computes the *entrywise* first and second order moments of the gradient, and uses them to adaptively normalize the gradient. In contrast, SING

		SGD	AdamW [28]	W+GC [51]	AdaBelief [60]	W+SING
ImageNet	ResNet18	72.44%	72.58%	72.31%	72.49%	72.93%
ImageNet	ResNet34	75.36%	75.29%	75.26%	75.49%	75.67%
CIFAR100	ResNet18	75.63%	77.95%	-	-	78.24%

Table 1: Top-1 accuracy classification results of ResNet [19] on CIFAR100 [24] and ImageNet [11] when trained from scratch. W+GC stands for the combination of AdamW [28] and Gradient Centralization [51] and W+SING stands for AdamW and SING. For CIFAR100, the results are averaged across five runs. The standard deviations (reported in the appendix) are sufficiently low to say that W+SING has a clear edge on AdamW. We do not report the mean and standard deviation on ImageNet-1K because we only launched each experiment once due to computational constraints but we can reasonably expect our results to be significant (see Figure 3 for a motivation).

first removes to the gradient its mean and divides it by its norm (standardization) prior to any further computations *at the layer level*. Furthermore, in Adam the first and second orders are averaged temporally while ours are not. Numerous variants of Adam have been proposed, mainly focusing on stabilizing the iterations of Adam. Notably, the popular AdamW [28] optimizer corrects how weight decay is applied in Adam, yielding a more robust method training larger models, for instance for training (visual) Transformers in practice [43]. Also in the panel of corrections to Adam, RAdam [26] proposes to fix the variance of adaptive learning rate by rewriting the update term, AdaBound [29] and AdaMod [13] clip the update, and AdaNorm [16] directly clips the gradient instead. Conversely, EAdam [54] and SAdam [42] target improving the ϵ term in the denominator. AdaBelief [60] is another variant of Adam. It computes an estimate of the standard deviation instead of the second order moment. AdaFactor [39] factorizes the elements of the gradient to reduce the memory consumption of the optimizer. The authors propose as well an analysis of the instabilities of Adam, and fixes. In this work, we also target reducing Adam’s instabilities via gradient standardization.

The works most closely related to ours are LARS [52] and LAMB [53]. Indeed, both optimizers normalize the gradient in a layer-wise fashion like us. However, both methods multiply the normalized gradient by the weight norm. This multiplication is undesired in our case as it would tame down our main theoretical result in Section 3 (Theorem 3.1) which is central to our work. Indeed, this theorem is the keystone to building a stable optimizer able to escape from narrow local minima using larger learning rates, whereas these methods leverage very large batch size to improve performance. Additionally, our method is hyperparameter-free in contrast to those of [52, 53]. Furthermore, these methods are new optimizers to be used as a replacement for Adam(W) whereas SING is a technique that can be used within any optimizer.

Other approaches leverage standardization to better train neural networks: Weight Standardization [36] and Weight Normalization [20, 38] parameterize the weights of the network to allow for a smoother training. While this affects the gradients, this approach is orthogonal to ours and could be used with our technique.

Another part of the literature focuses on improving the stability of training processes to ensure smoother convergence. Notably, techniques such as LookAhead [57] adopt an approach where weights computed over the previous k iterations are averaged. Similarly, Gradient Centralization [51] involves subtracting the mean of the gradient, effectively reducing its ℓ^2 norm. In our work, we draw upon these techniques, but it is important to highlight that our approach is distinct and independent from this line of research.

Lastly, it is common in non-convex optimization to normalize the gradient descent algorithm [9, 32, 59]. This line of work supports that the standardization strategies is a simple way to find a better minimizer. In this work, we translate this strategy to deep learning.

5 Experiments

In this section, we evaluate SING on classification, depth estimation and natural language processing. We run all the experiments on a single Tesla V100 GPU with 32GB of VRAM. The code to reproduce the results will be made available upon publication.

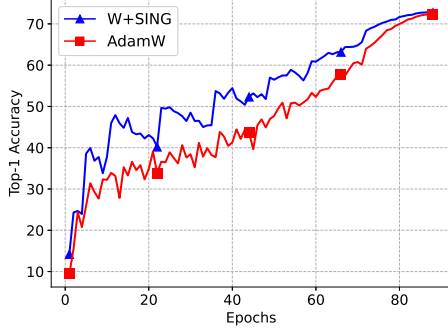


Figure 3: Evolution of the accuracy throughout training on ImageNet-1K with a ResNet18. The almost-periodic oscillation of the metric is typical of SING, and could be explained by the large steps taken by the optimizer. As illustrated in Figure 1, at the beginning the learning rate is very high to avoid local minima and is slowly reduced to reach convergence.

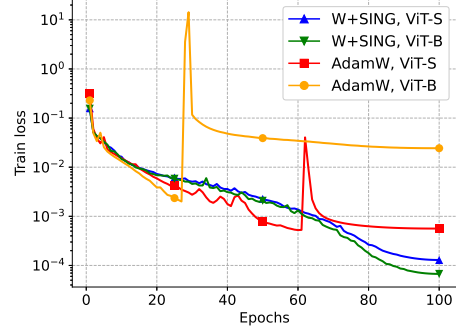


Figure 4: An illustration of a failure case of Adam when trained on ViT-small. The train loss suddenly spikes during training, reducing the final performance. The learning rate scheduler is a cosine decay, hence the learning rate is already small when the explosion occurs.

	Maximum LR	AdamW [28]	AdamW + SING
ViT-S [14]	0.05	78.13%	96.56%
ViT-S [14] (\pm Normalization)	NC	93.00% (+14.87%)	NC
ViT-S [14] (\pm GC [51])	0.01 (1/5)	77.46% (-0.67%)	93.86% (-2.70%)
ViT-S [14] (\pm LookAhead [57])	0.01 (1/5)	54.79% (-23.35%)	95.63% (-0.93%)
ViT-S [14] (\pm Softplus [42])	0.005 (1/10)	NC	89.38% (-7.18%)
ViT-B [14]	0.05	NC	97.15%

Table 2: Ablation study of the different components of SING using a ViT-S on RDE. The reported metric is the accuracy. Each component allow for a higher learning rate. For AdamW, we added the component and studied the convergence. For AdamW + SING, we removed it. As the theory suggests, the higher the learning rate, the higher the final performance. NC stands for no convergence *i.e.* the loss could not be stabilized throughout the iterations. The maximum LR reported corresponds to the one for AdamW + SING. As displayed in Figure 4, the training of ViT-B spiked resulting in irrelevant performance. For AdamW, unstable nature of the training largely widens the gaps in performance when adding a component. In all cases, the best LR using AdamW alone was 10^{-3} .

5.1 Image classification

We evaluate our technique on the large-scale ImageNet-1K dataset [11] which consists of 1.28 million images for training and 50K images for validation from 1000 categories. We use the FFCV library [25] and its recipe: the data augmentation consists in random horizontal flips and random resized crops. Notably, the downsampling layers are replaced by BlurPool [58]. The size of the images is 192×192 during training and 224×224 at evaluation [44]. Our networks are trained for 88 epochs with a batch size of 1024. The loss to be minimized is the cross-entropy with a label smoothing [40] of 0.1. For all networks, there is a 5-epoch linear warmup and a cosine decaying schedule afterward.

We carefully design our hyper-parameter tuning strategy to ensure a fair comparison. First, we tune the learning rate among limited values: $\{5 \times 10^{-4}, 10^{-3}, 5 \times 10^{-3}, 10^{-2}\}$ for AdamW and $\{5 \times 10^{-3}, 10^{-2}, 5 \times 10^{-2}, 10^{-1}\}$ for SING used within AdamW. In the rare cases where the best learning rate found is one of the extreme value of the set, additional learning rates were tested. For all networks and optimizers the best learning rate found is the last one before the training explodes. Then, we tune the weight decay using the best learning rate found. The values assessed for the weight decay are $\{5 \times 10^{-4}, 5 \times 10^{-3}, 5 \times 10^{-2}, 5 \times 10^{-1}\}$. Finally, the results are reported in Table 1. We notice that SING combined with AdamW systematically outperforms AdamW. The evolution of the

	SGD	AdamW [28]	AdaBelief [60]	AdaFactor [39]
w/o SING	0.25%	78.13%	60.26%	74.98%
w/ SING	94.25% (+94.23%)	96.56% (+18.43%)	96.70% (+36.44%)	76.26% (+1.28%)

Table 3: Combination of SING with other optimizers for training a ViT-S [14] model on RDE. Note that SGD barely works on this task and model despite the hyper-parameter tuning. We argue that its performance could be further improved by tuning the momentum hyper-parameter. See the Appendix for more details. We notice that for three out of four optimizers, incorporating SING helps improve the performance. See the Appendix for more details.

accuracy throughout training can be seen in Figure 3. SING seems to outperform AdamW during the entire training, but seem to loose its edge at the end of the training. We leave the study of this phenomena for future works.

Additionally, we trained a ResNet18 on CIFAR100 [24], which consists of 50K training images and 10K testing images from 100 classes. The images are of size 32×32 . The network was trained for 300 epochs using a batch size of 128. The learning rate scheduler and the tuning strategy are the same than for ImageNet. The results are visible in Table 1. We see that even in this challenging setting, the combination of AdamW and SING outperforms AdamW and SGD.

5.2 Depth Estimation

In this section, we investigate the performance of our optimizer on a depth estimation task using a synthetic dataset. The RDE dataset [8] consists of 50K 128×128 images of rectangles randomly placed within an image. Depth naturally arises as rectangles are placed on top of each other. The goal is to predict the depth for each pixel in the image, depending on which rectangle it belongs too. This task is interesting because although there exists a simple algorithm that computes the desired depth with 100% accuracy, neural networks struggle to get good performance. Notably, we found training a ViT-small [14] on this task in an image-to-image fashion to be particularly challenging using AdamW. For usual learning rates, the loss spikes randomly during training, largely lowering the final performance. See Figure 4 for more details. For very small learning rates, the training loss doesn’t decrease fast enough to get results in a reasonable amount of time. In this case, we found using SING with AdamW to be a good choice as the normalization prevents the gradient from exploding during training. As a result, the combination of AdamW and SING outperformed AdamW by a large margin. The larger the assessed model, the worse the instabilities. ViT-big [14] does not converge when using AdamW. We tried several sets of hyper-parameters to draw this conclusion.

We used the same hyper-parameter tuning strategy and learning rate scheduler as for ImageNet-1K. The network was trained for 100 epochs using a batch size of 512. The loss we minimized was the MSE. See Table 2 for the results and an ablation study. The ablation study shows that each component of SING helps to achieve a higher learning rate and therefore higher performance. Notably, softplus [42] seems to largely help SING while it is detrimental for AdamW. The normalization seems to be a determining factor for reaching convergence although it does not fully explain the success of SING. We also studied the impact of SING when combined with other optimizers. The results are visible in Table 3. We used all methods with their default hyper-parameters except for SGD where we tried different values for the momentum. We see that for three out of the four assessed optimizers, the variant with SING significantly outperforms its counterpart. For AdaFactor [39] there is barely any performance gain. We claim this is due to the numerous tweaks within the optimizer that have been tailored for a gradient descent without SING.

5.3 Natural language processing

In this section, we evaluate the performance of our optimizer on natural language processing tasks. First, we trained a Transformer with pre-norm convention [47] on the IWSLT14 German-to-English (De-En) dataset [5] using the FAIRSEQ [33] library. We used the code of AdaHessian [50] as is but surprisingly we were not able to reproduce the results reported for AdamW. Instead, we used the hyper-parameters reported in [48] and found them to be better, but still below the announced results. Then, we used Hugging Face TRANSFORMERS library [46] to fine-tune Bert [12] on the SQuAD

			AdamW [28]	AdamW + SING
IWSLT14	From scratch	Transformer [45]	34.76	35.41
SQuAD ¹	Fine-tuning	Bert [12]	80.53% / 88.39%	81.00% / 88.34%
SWAG ¹	Fine-tuning	RoBERTa [27]	80.45%	83.33%

Table 4: First line: BLUE score on the IWSLT14 task, when training a SMALL Transformer [33] from scratch. Second line: Fine-tuning results on the SQuAD dataset [37]; the reported values are the proportion of exact matches and the F1 score. Third line: Fine-tuning results on the SWAG dataset [56]; the reported value is the accuracy.

dataset [37] and RoBERTa on SWAG [56]. The results are reported in Table 4. In all cases, the combination of AdamW and SING outperforms a well-tuned AdamW.

We noticed that the gradient norm was increasing throughout training. After investigation, it turned out the culprits were the weights and biases of the Layer Normalization [2] layers. We decided to disable the learning of these weights and found the performance of both optimizers to be improved. We claim doing so is not problematic in practice as disabling the learning of these parameters have been pointed out as beneficial in the literature [49].

5.4 Limitations

We tried SING on other tasks such as image denoising, where the models trained with SING attained the same performance of AdamW, but did not result in improved results. This suggests SING’s effectiveness can vary depending on the task and architecture. Additionally, we found our optimizer to not work well when used in conjunction with LayerNorm [2] or LayerScale [43]. While a simple fix is to disable the learning of these weights, it raises the question of why and calls for a better solution. Finally, we propose a convergence proof of the iterates defined in 2, which does not incorporate AdamW even though we mainly used their combination in the paper.

6 Conclusion

We introduced SING, a plug-and-play technique that improves the stability and generalization of the Adam(W) optimizer in deep learning, and can be used with any optimizer. By leveraging layer-wise gradient standardization, SING enhances the performance of the optimizer without introducing additional hyperparameters. Extensive experimentation across various tasks demonstrates its effectiveness compared to the original AdamW optimizer. Theoretical analysis reveals that SING enables the optimizer to escape narrow local minima within a single step, with the required learning rate inversely proportional to the network’s depth. This compatibility with deep neural networks highlights its practicality. The analysis also provides valuable insights into the behavior of SING, such as its convergence rate or stability, and its advantages over traditional optimization techniques.

In conclusion, our proposed SING technique offers a practical and effective upgrade to the Adam(W) optimizer in deep learning. By enhancing stability and generalization, it contributes to the improvement of optimization algorithms in neural network training. The results of our research, combined with the theoretical analysis, open avenues for further exploration, including investigating the compatibility of SING with other optimization frameworks and addressing the challenges associated with specific normalization techniques.

Acknowledgements. This work was supported by grants from Région Ile-de-France, the DGA Astrid Maturation project SURECAVI ANR-21-ASM3-0002, the Office of Naval research grant N00014-17-1-2552, and the ANR project IMPROVED ANR-22-CE39-0006-04. This work was performed using HPC resources from GENCI-IDRIS (grants 2023-AD011012453R2, 2023-AD011012458R2). Centre Borelli is also with Université Paris Cité, SSA and INSERM.

¹We took the code of Hugging Face (<https://huggingface.co/transformers/v2.3.0/examples.html>) as is and launched it, and found the performance to be lower than announced. More details in Appendix.

References

- [1] Abien Fred Agarap. Deep learning using rectified linear units (relu). *arXiv preprint arXiv:1803.08375*, 2018.
- [2] Jimmy Lei Ba, Jamie Ryan Kiros, and Geoffrey E Hinton. Layer normalization. *arXiv preprint arXiv:1607.06450*, 2016.
- [3] Sunitha Basodi, Chunyan Ji, Haiping Zhang, and Yi Pan. Gradient amplification: An efficient way to train deep neural networks. *Big Data Mining and Analytics*, 3(3):196–207, 2020.
- [4] Joy Buolamwini and Timnit Gebru. Gender shades: Intersectional accuracy disparities in commercial gender classification. In *Conference on fairness, accountability and transparency*, pages 77–91. PMLR, 2018.
- [5] Mauro Cettolo, Jan Niehues, Sebastian Stüker, Luisa Bentivogli, and Marcello Federico. Report on the 11th iwslt evaluation campaign. In *Proceedings of the 11th International Workshop on Spoken Language Translation: Evaluation Campaign*, pages 2–17, 2014.
- [6] Aakanksha Chowdhery, Sharan Narang, Jacob Devlin, Maarten Bosma, Gaurav Mishra, Adam Roberts, Paul Barham, Hyung Won Chung, Charles Sutton, Sebastian Gehrmann, et al. Palm: Scaling language modeling with pathways. *arXiv preprint arXiv:2204.02311*, 2022.
- [7] Yaim Cooper. The loss landscape of overparameterized neural networks. *arXiv preprint arXiv:1804.10200*, 2018.
- [8] Adrien Courtois, Jean-Michel Morel, and Pablo Arias. Investigating neural architectures by synthetic dataset design. In *Proceedings of the IEEE/CVF Conference on Computer Vision and Pattern Recognition*, pages 4890–4899, 2022.
- [9] Ashok Cutkosky and Harsh Mehta. Momentum improves normalized sgd. In *International conference on machine learning*, pages 2260–2268. PMLR, 2020.
- [10] Alexandre Défossez, Léon Bottou, Francis Bach, and Nicolas Usunier. A simple convergence proof of adam and adagrad. *arXiv preprint arXiv:2003.02395*, 2020.
- [11] Jia Deng, Wei Dong, Richard Socher, Li-Jia Li, Kai Li, and Li Fei-Fei. Imagenet: A large-scale hierarchical image database. In *2009 IEEE conference on computer vision and pattern recognition*, pages 248–255. Ieee, 2009.
- [12] Jacob Devlin, Ming-Wei Chang, Kenton Lee, and Kristina Toutanova. Bert: Pre-training of deep bidirectional transformers for language understanding. *arXiv preprint arXiv:1810.04805*, 2018.
- [13] Jianbang Ding, Xuancheng Ren, Ruixuan Luo, and Xu Sun. An adaptive and momental bound method for stochastic learning. *arXiv preprint arXiv:1910.12249*, 2019.
- [14] Alexey Dosovitskiy, Lucas Beyer, Alexander Kolesnikov, Dirk Weissenborn, Xiaohua Zhai, Thomas Unterthiner, Mostafa Dehghani, Matthias Minderer, Georg Heigold, Sylvain Gelly, et al. An image is worth 16x16 words: Transformers for image recognition at scale. *arXiv preprint arXiv:2010.11929*, 2020.
- [15] Timothy Dozat. Incorporating nesterov momentum into adam. *ICLR 2016 Workshop*, 2016.
- [16] Shiv Ram Dubey, Satish Kumar Singh, and Bidyut Baran Chaudhuri. Adanorm: Adaptive gradient norm correction based optimizer for cnns. In *Proceedings of the IEEE/CVF Winter Conference on Applications of Computer Vision*, pages 5284–5293, 2023.
- [17] Ian J Goodfellow, Oriol Vinyals, and Andrew M Saxe. Qualitatively characterizing neural network optimization problems. *arXiv preprint arXiv:1412.6544*, 2014.
- [18] Haowei He, Gao Huang, and Yang Yuan. Asymmetric valleys: Beyond sharp and flat local minima. *Advances in neural information processing systems*, 32, 2019.

- [19] Kaiming He, Xiangyu Zhang, Shaoqing Ren, and Jian Sun. Deep residual learning for image recognition. In *Proceedings of the IEEE conference on computer vision and pattern recognition*, pages 770–778, 2016.
- [20] Lei Huang, Xianglong Liu, Yang Liu, Bo Lang, and Dacheng Tao. Centered weight normalization in accelerating training of deep neural networks. In *Proceedings of the IEEE International Conference on Computer Vision*, pages 2803–2811, 2017.
- [21] Sergey Ioffe and Christian Szegedy. Batch normalization: Accelerating deep network training by reducing internal covariate shift. In *International conference on machine learning*, pages 448–456. pmlr, 2015.
- [22] Nitish Shirish Keskar, Dheevatsa Mudigere, Jorge Nocedal, Mikhail Smelyanskiy, and Ping Tak Peter Tang. On large-batch training for deep learning: Generalization gap and sharp minima. *arXiv preprint arXiv:1609.04836*, 2016.
- [23] Diederik P. Kingma and Jimmy Ba. Adam: A method for stochastic optimization. In Yoshua Bengio and Yann LeCun, editors, *Int. Conf. on Learning Representations*, 2015.
- [24] Alex Krizhevsky, Geoffrey Hinton, et al. Learning multiple layers of features from tiny images, 2009.
- [25] Guillaume Leclerc, Andrew Ilyas, Logan Engstrom, Sung Min Park, Hadi Salman, and Aleksander Madry. FFCV: Accelerating training by removing data bottlenecks. <https://github.com/libffcv/ffcv/>, 2022. commit 2544abd.
- [26] Liyuan Liu, Haoming Jiang, Pengcheng He, Weizhu Chen, Xiaodong Liu, Jianfeng Gao, and Jiawei Han. On the variance of the adaptive learning rate and beyond. *arXiv preprint arXiv:1908.03265*, 2019.
- [27] Yinhan Liu, Myle Ott, Naman Goyal, Jingfei Du, Mandar Joshi, Danqi Chen, Omer Levy, Mike Lewis, Luke Zettlemoyer, and Veselin Stoyanov. Roberta: A robustly optimized bert pretraining approach. *arXiv preprint arXiv:1907.11692*, 2019.
- [28] Ilya Loshchilov and Frank Hutter. Decoupled weight decay regularization. *arXiv preprint arXiv:1711.05101*, 2017.
- [29] Liangchen Luo, Yuanhao Xiong, Yan Liu, and Xu Sun. Adaptive gradient methods with dynamic bound of learning rate. *arXiv preprint arXiv:1902.09843*, 2019.
- [30] Agnes Lydia and Sagayaraj Francis. Adagrad—an optimizer for stochastic gradient descent. *Int. J. Inf. Comput. Sci.*, 6(5):566–568, 2019.
- [31] Igor Molybog, Peter Albert, Moya Chen, Zachary DeVito, David Esiobu, Naman Goyal, Punit Singh Koura, Sharan Narang, Andrew Poulton, Ruan Silva, et al. A theory on adam instability in large-scale machine learning. *arXiv preprint arXiv:2304.09871*, 2023.
- [32] Ryan Murray, Brian Swenson, and Soumya Kar. Revisiting normalized gradient descent: Fast evasion of saddle points. *IEEE Transactions on Automatic Control*, 64(11):4818–4824, 2019.
- [33] Myle Ott, Sergey Edunov, Alexei Baevski, Angela Fan, Sam Gross, Nathan Ng, David Grangier, and Michael Auli. fairseq: A fast, extensible toolkit for sequence modeling. *arXiv preprint arXiv:1904.01038*, 2019.
- [34] Razvan Pascanu, Tomas Mikolov, and Yoshua Bengio. On the difficulty of training recurrent neural networks. In *International conference on machine learning*, pages 1310–1318. Pmlr, 2013.
- [35] Jeffrey Pennington and Yasaman Bahri. Geometry of neural network loss surfaces via random matrix theory. In *International Conference on Machine Learning*, pages 2798–2806. PMLR, 2017.
- [36] Siyuan Qiao, Huiyu Wang, Chenxi Liu, Wei Shen, and Alan Yuille. Micro-batch training with batch-channel normalization and weight standardization. *arXiv preprint arXiv:1903.10520*, 2019.

- [37] Pranav Rajpurkar, Jian Zhang, Konstantin Lopyrev, and Percy Liang. Squad: 100,000+ questions for machine comprehension of text. *arXiv preprint arXiv:1606.05250*, 2016.
- [38] Tim Salimans and Durk P Kingma. Weight normalization: A simple reparameterization to accelerate training of deep neural networks. *Advances in neural information processing systems*, 29, 2016.
- [39] Noam Shazeer and Mitchell Stern. Adafactor: Adaptive learning rates with sublinear memory cost. In *International Conference on Machine Learning*, pages 4596–4604. PMLR, 2018.
- [40] Christian Szegedy, Vincent Vanhoucke, Sergey Ioffe, Jon Shlens, and Zbigniew Wojna. Re-thinking the inception architecture for computer vision. In *Proceedings of the IEEE conference on computer vision and pattern recognition*, pages 2818–2826, 2016.
- [41] T. Tieleman and G. Hinton. Lecture 6.5 - rmsprop, coursera: Neural networks for machine learning., 2012. Technical report.
- [42] Qianqian Tong, Guannan Liang, and Jinbo Bi. Calibrating the adaptive learning rate to improve convergence of adam. *Neurocomputing*, 481:333–356, 2022.
- [43] Hugo Touvron, Matthieu Cord, Alexandre Sablayrolles, Gabriel Synnaeve, and Hervé Jégou. Going deeper with image transformers. In *Proceedings of the IEEE/CVF International Conference on Computer Vision*, pages 32–42, 2021.
- [44] Hugo Touvron, Andrea Vedaldi, Matthijs Douze, and Hervé Jégou. Fixing the train-test resolution discrepancy. *Advances in neural information processing systems*, 32, 2019.
- [45] Ashish Vaswani, Noam Shazeer, Niki Parmar, Jakob Uszkoreit, Llion Jones, Aidan N. Gomez, Lukasz Kaiser, and Illia Polosukhin. Attention is all you need. In *Advances in Neural Information Processing Systems*, 2017.
- [46] Thomas Wolf, Lysandre Debut, Victor Sanh, Julien Chaumond, Clement Delangue, Anthony Moi, Pierric Cistac, Tim Rault, Rémi Louf, Morgan Funtowicz, Joe Davison, Sam Shleifer, Patrick von Platen, Clara Ma, Yacine Jernite, Julien Plu, Canwen Xu, Teven Le Scao, Sylvain Gugger, Mariama Drame, Quentin Lhoest, and Alexander M. Rush. Transformers: State-of-the-art natural language processing. In *Proceedings of the 2020 Conference on Empirical Methods in Natural Language Processing: System Demonstrations*, pages 38–45, Online, October 2020. Association for Computational Linguistics.
- [47] Ruibin Xiong, Yunchang Yang, Di He, Kai Zheng, Shuxin Zheng, Chen Xing, Huishuai Zhang, Yanyan Lan, Liwei Wang, and Tiejun Liu. On layer normalization in the transformer architecture. In *International Conference on Machine Learning*, pages 10524–10533. PMLR, 2020.
- [48] Haoran Xu, Benjamin Van Durme, and Kenton Murray. Bert, mbert, or bibert? a study on contextualized embeddings for neural machine translation. *arXiv preprint arXiv:2109.04588*, 2021.
- [49] Jingjing Xu, Xu Sun, Zhiyuan Zhang, Guangxiang Zhao, and Junyang Lin. Understanding and improving layer normalization. *Advances in Neural Information Processing Systems*, 32, 2019.
- [50] Zhewei Yao, Amir Gholami, Sheng Shen, Mustafa Mustafa, Kurt Keutzer, and Michael Mahoney. Adahessian: An adaptive second order optimizer for machine learning. In *proceedings of the AAAI conference on artificial intelligence*, volume 35, pages 10665–10673, 2021.
- [51] Hongwei Yong, Jianqiang Huang, Xiansheng Hua, and Lei Zhang. Gradient centralization: A new optimization technique for deep neural networks. In *Computer Vision–ECCV 2020: 16th European Conference, Glasgow, UK, August 23–28, 2020, Proceedings, Part I 16*, pages 635–652. Springer, 2020.
- [52] Yang You, Igor Gitman, and Boris Ginsburg. Large batch training of convolutional networks. *arXiv preprint arXiv:1708.03888*, 2017.
- [53] Yang You, Jing Li, Sashank Reddi, Jonathan Hseu, Sanjiv Kumar, Srinadh Bhojanapalli, Xiaodan Song, James Demmel, Kurt Keutzer, and Cho-Jui Hsieh. Large batch optimization for deep learning: Training bert in 76 minutes. *arXiv preprint arXiv:1904.00962*, 2019.

- [54] Wei Yuan and Kai-Xin Gao. Eadam optimizer: How ϵ impact adam. *arXiv preprint arXiv:2011.02150*, 2020.
- [55] Manzil Zaheer, Sashank Reddi, Devendra Sachan, Satyen Kale, and Sanjiv Kumar. Adaptive methods for nonconvex optimization. *Advances in neural information processing systems*, 31, 2018.
- [56] Rowan Zellers, Yonatan Bisk, Roy Schwartz, and Yejin Choi. Swag: A large-scale adversarial dataset for grounded commonsense inference. *arXiv preprint arXiv:1808.05326*, 2018.
- [57] Michael Zhang, James Lucas, Jimmy Ba, and Geoffrey E Hinton. Lookahead optimizer: k steps forward, 1 step back. *Advances in neural information processing systems*, 32, 2019.
- [58] Richard Zhang. Making convolutional networks shift-invariant again. In *International conference on machine learning*, pages 7324–7334. PMLR, 2019.
- [59] Shen-Yi Zhao, Yin-Peng Xie, and Wu-Jun Li. On the convergence and improvement of stochastic normalized gradient descent. *Science China Information Sciences*, 64:1–13, 2021.
- [60] Juntang Zhuang, Tommy Tang, Yifan Ding, Sekhar C Tatikonda, Nicha Dvornek, Xenophon Papademetris, and James Duncan. Adabelief optimizer: Adapting stepsizes by the belief in observed gradients. *Advances in neural information processing systems*, 33:18795–18806, 2020.

A Theorems & Proofs

Theorem 3.2. The iterates defined by (2) are invariant w.r.t. transformation (6), and preserve the mean (7).

Proof. The first property is satisfied thanks to the normalization. Indeed, consider the iterates

$$y_{t+1} = y_t - \eta \frac{\phi(\nabla \tilde{F}(y_t))}{\Gamma(\phi(\nabla \tilde{F}(y_t)))},$$

where \tilde{F} is defined in (6). Hence,

$$y_{t+1} = y_t - \eta \frac{\phi(\nabla \alpha F(y_t))}{\Gamma(\phi(\alpha \nabla F(y_t)))},$$

Since ϕ and Γ are both homogeneous operators,

$$y_{t+1} = y_t - \eta \frac{\alpha \phi(\nabla F(y_t))}{\alpha \Gamma(\phi(\nabla F(y_t)))} = y_t - \eta \frac{\phi(\nabla F(y_t))}{\Gamma(\phi(\nabla F(y_t)))}.$$

Therefore, we have the property $y_t = x_t$ (2). Moreover, define the mean operator $m(x) = \frac{1}{p} \sum_{i=1}^p x_i$. For $z \in \mathbb{R}^p$, we have

$$m\left(\frac{\phi(z)}{\Gamma(\phi(z))}\right) = \frac{1}{p} \sum_{k=1}^D \frac{1}{\|\phi(z_{I_k})\|_2} \sum_{l \in I_k} [\phi(z)]_l = 0,$$

where the last inequality comes from the definition of the gradient centralization operation ϕ . Hence, since $m(\cdot)$ is a linear function,

$$\begin{aligned} m(x_{t+1}) &= m\left(x_t - \eta \frac{\phi(\nabla F(x_t))}{\Gamma(\phi(\nabla F(x_t)))}\right), \\ &= m(x_t) - \eta m\left(\frac{\phi(\nabla F(x_t))}{\Gamma(\phi(\nabla F(x_t)))}\right), \\ &= m(x_t). \end{aligned}$$

□

Theorem 3.3 (Convergence without gradient centralization). Let assumptions (8) and (9) hold. Assume the gradient is computed across a mini-batch of size $B = \frac{\sigma^2}{\epsilon^2}$. Let x_t be the sequence of iterates (2) with $\phi = I$. Then, we have

$$\frac{1}{T} \sum_{t=0}^{T-1} \mathbb{E}[\|\nabla F(x_t)\|_2] \leq \frac{F(x_0)}{\eta T} + (1 + \sqrt{D})\epsilon + \frac{\eta LD}{2}. \quad (10)$$

If we set $\tau \sim \mathcal{U}([0, T-1])$, $\eta = \frac{2\epsilon}{L}$ and $T = \frac{LF(x_0)}{2\epsilon^2}$, we obtain $\mathbb{E}[\|\nabla F(x_\tau)\|_2] \leq (2 + \sqrt{D} + D)\epsilon$. Therefore, the iteration complexity and computation complexity to achieve an ϵ -stationary point are $\mathcal{O}(1/\epsilon^2)$ and $\mathcal{O}(1/\epsilon^4)$, respectively.

Before proving this theorem, we will introduce and prove two technical lemmas.

Lemma A.1. For every $x \in \mathbb{R}^p$, the following equality holds

$$\left\| \frac{x}{\Gamma(x)} \right\|_2 = \sqrt{D}.$$

Proof. The function Γ is block-wise constant such that

$$\forall k \in [1, D], \forall i \in I_k, [\Gamma(x)]_i = \|x_{I_k}\|_2 = \sqrt{\sum_{j \in I_k} [x]_j^2}.$$

Hence

$$\begin{aligned}
\left\| \frac{x}{\Gamma(x)} \right\|_2^2 &= \sum_{j=1}^d \left[\frac{x}{\Gamma(x)} \right]_j^2 = \sum_{k=1}^D \sum_{i \in I_k} \frac{[x]_i^2}{[\Gamma(x)]_i^2} \\
&= \sum_{k=1}^D \sum_{i \in I_k} \frac{[x]_i^2}{\|x_{I_k}\|_2^2} = \sum_{k=1}^D \frac{\|x_{I_k}\|_2^2}{\|x_{I_k}\|_2^2} \\
&= D.
\end{aligned}$$

□

Lemma A.2. For every $x \in \mathbb{R}^p$, the following equality holds

$$\left\langle x, \frac{x}{\Gamma(x)} \right\rangle = \sum_{k=1}^D \|x_{I_k}\|_2 \stackrel{\text{def}}{=} N(x).$$

In particular, we have

$$\|x\|_2 \leq N(x).$$

Proof. The first part of the lemma can be derived directly using the same notation as for Lemma A.1:

$$\begin{aligned}
\left\langle x, \frac{x}{\Gamma(x)} \right\rangle &= \sum_{j=1}^d \frac{[x]_j^2}{[\Gamma(x)]_j} = \sum_{k=1}^D \sum_{i \in I_k} \frac{[x]_i^2}{\|x_{I_k}\|_2} \\
&= \sum_{k=1}^D \frac{\|x_{I_k}\|_2^2}{\|x_{I_k}\|_2} = \sum_{k=1}^D \|x_{I_k}\|_2.
\end{aligned}$$

The second part can be shown using the fact that $\|z\|_2 \leq \|z\|_1$ for every $z \in \mathbb{R}^D$. We define $z \in \mathbb{R}^D$ such that

$$\forall k \in \llbracket 1, D \rrbracket, z_k = \|x_{I_k}\|_2,$$

then $\|z\|_1 = N(x)$ and

$$\|z\|_2^2 = \sum_{k=1}^D \|x_{I_k}\|_2^2 = \sum_{k=1}^D \sum_{i \in I_k} [x]_i^2 = \sum_{j=1}^d [x]_j^2 = \|x\|_2^2.$$

□

Now, onto the proof of Theorem 3.3.

Proof. We note ∇f the stochastic approximation of the real gradient ∇F and we assume that the stochastic gradient has a σ -bounded variance ($\sigma > 0$) i.e.

$$\forall x \in \mathbb{R}^p, \mathbb{E} [\|\nabla F(x) - \nabla f(x)\|_2^2] \leq \sigma^2, \quad (12)$$

and that the gradient of F is L -Lipschitz such that

$$F(x_+) \leq F(x) + \langle \nabla F(x), x_+ - x \rangle + \frac{L}{2} \|x_+ - x\|_2^2. \quad (13)$$

When $\phi = I$, the gradient updates are given by

$$x_+ = x - \eta \frac{\nabla f(x)}{\Gamma(\nabla f(x))}, \quad (14)$$

where the division is element-wise. Then, using (13) with the updates defined in (14):

$$\begin{aligned}
F(x_+) &\leq F(x) - \eta \left\langle \nabla F(x), \frac{\nabla f(x)}{\Gamma(\nabla f(x))} \right\rangle + \eta^2 \frac{L}{2} \left\| \frac{\nabla f(x)}{\Gamma(\nabla f(x))} \right\|_2^2 \\
&\leq F(x) - \eta \left\langle \nabla F(x) - \nabla f(x), \frac{\nabla f(x)}{\Gamma(\nabla f(x))} \right\rangle - \eta \left\langle \nabla f(x), \frac{\nabla f(x)}{\Gamma(\nabla f(x))} \right\rangle + \frac{\eta^2 LD}{2} \\
&\leq F(x) + \eta \sqrt{D} \|\nabla F(x) - \nabla f(x)\|_2 - \eta N(\nabla f(x)) + \frac{\eta^2 LD}{2}, \quad (15)
\end{aligned}$$

where the last inequality comes from the Cauchy-Schwartz inequality used with Lemma A.1 and the first part of Lemma A.2. Using the second part of Lemma A.2, we get

$$\|\nabla F(x)\|_2 \leq \|\nabla F(x) - \nabla f(x)\|_2 + \|\nabla f(x)\|_2 \leq \|\nabla F(x) - \nabla f(x)\|_2 + N(\nabla f(x)). \quad (16)$$

Upper-bounding $N(\nabla f(x))$ using (15) gives us

$$\|\nabla F(x)\|_2 \leq \frac{F(x) - F(x_+)}{\eta} + (1 + \sqrt{D}) \|\nabla F(x) - \nabla f(x)\|_2 + \frac{\eta LD}{2}. \quad (17)$$

Then, if $\nabla f(x)$ is the average of $B = \frac{\sigma^2}{\epsilon^2}$ gradient approximations over a mini-batch, we get

$$\mathbb{E}[\|\nabla F(x) - \nabla f(x)\|_2] \leq \sqrt{\mathbb{E}[\|\nabla F(x) - \nabla f(x)\|_2^2]} \leq \frac{\sigma}{B} = \epsilon. \quad (18)$$

Taking the expectation in (17) for $x_+ = x_{t+1}$ and $x = x_t$ for a given $t \in \mathbb{N}$ and $(x_t)_{t \in \mathbb{N}}$ being the updates defined by (14), we get

$$\begin{aligned} \frac{1}{T} \sum_{t=0}^{T-1} \|\nabla F(x_t)\|_2 &\leq \frac{F(x_0) - F(x_T)}{\eta T} + \frac{1 + \sqrt{D}}{T} \sum_{t=0}^{T-1} \mathbb{E}[\|\nabla F(x_t) - \nabla f(x_t)\|_2] + \frac{\eta LD}{2} \\ &\leq \frac{F(x_0)}{\eta T} + (1 + \sqrt{D})\epsilon + \frac{\eta LD}{2}. \end{aligned}$$

The last inequality comes from (18) and the assumption that $F \geq 0$. This shows the first part of the theorem. Now, if we let $\eta = \frac{2\epsilon}{L}$ and $T = \frac{LF(x_0)}{2\epsilon^2}$ we get

$$\frac{1}{T} \sum_{t=0}^{T-1} \|\nabla F(x_t)\|_2 \leq (2 + \sqrt{D} + D)\epsilon. \quad (19)$$

□

Theorem 3.4 (Convergence with gradient centralization). Let assumptions (8) and (9) hold. Assume the gradient is computed across a mini-batch of size $B = \frac{\sigma^2}{\epsilon^2}$. Let x_t be the sequence of iterates (2). Then we have

$$\frac{1}{T} \sum_{t=0}^{T-1} \mathbb{E}[\|\nabla F(x_t)\|_\phi] \leq \frac{F(x_0)}{\eta T} + (1 + \sqrt{D})\epsilon + \frac{\eta LD}{2}, \quad (11)$$

where $\|\cdot\|_\phi^2 = \langle \cdot, \phi(\cdot) \rangle_2$ is a pseudo-norm. If we set $\tau \sim \mathcal{U}([0, T-1])$, $\eta = \frac{2\epsilon}{L}$ and $T = \frac{LF(x_0)}{2\epsilon^2}$, we obtain $\mathbb{E}[\|\nabla F(x_\tau)\|_\phi] \leq (2 + \sqrt{D} + D)\epsilon$. Therefore, the iteration complexity and computation complexity to achieve an (ϵ, ϕ) -stationary point are $\mathcal{O}(1/\epsilon^2)$ and $\mathcal{O}(1/\epsilon^4)$, respectively.

As for the proof of Theorem 3.3, we start by introducing and proving two technical lemmas.

Lemma A.3. For every $x \in \mathbb{R}^p$, the following equality holds

$$\left\| \frac{\phi(x)}{\Gamma(\phi(x))} \right\|_2 = \sqrt{D}.$$

Proof. The proof is direct using Lemma A.1 with $x = \phi(z)$. □

Lemma A.4. For every $x \in \mathbb{R}^p$, the following inequality holds

$$\left\langle x, \frac{\phi(x)}{\Gamma(\phi(x))} \right\rangle = \sum_{k=1}^D \|x_{I_k}\|_\phi \stackrel{\text{def}}{=} N_\phi(x),$$

where $\|\cdot\|_\phi \stackrel{\text{def}}{=} \langle \cdot, \phi(\cdot) \rangle$ is pseudo-norm. In particular, we have

$$\|x\|_\phi \leq \|x\|_2, \quad \text{and} \quad \|x\|_\phi \leq N_\phi(x).$$

Proof. As for the other lemmas, the first part is direct

$$\begin{aligned}
\left\langle x, \frac{\phi(x)}{\Gamma(\phi(x))} \right\rangle &= \sum_{j=1}^d [x]_j \frac{[\phi(x)]_j}{[\Gamma(\phi(x))]_j} = \sum_{k=1}^D \sum_{i \in I_k} [x]_i \frac{[\phi(x)]_i}{[\Gamma(\phi(x))]_i} \\
&= \sum_{k=1}^D \frac{1}{\|\phi(x_{I_k})\|_2} \sum_{i \in I_k} [x]_i [\phi(x)]_i = \sum_{k=1}^D \frac{\langle x_{I_k}, \phi(x_{I_k}) \rangle}{\|\phi(x_{I_k})\|_2} \\
&= \sum_{k=1}^D \sqrt{\langle x_{I_k}, \phi(x_{I_k}) \rangle} = \sum_{k=1}^D \|x_{I_k}\|_\phi.
\end{aligned}$$

The penultimate inequality comes from the fact that ϕ is self-adjoint and such that $\phi \circ \phi = \phi$:

$$\|\phi(x)\|_2^2 = \langle \phi(x), \phi(x) \rangle = \langle x, \phi(\phi(x)) \rangle = \langle x, \phi(x) \rangle.$$

The Cauchy-Schwartz inequality applied on the above equality gives us the second part of the lemma:

$$\|\phi(x)\|_2^2 \leq \|x\|_2 \|\phi(x)\|_2,$$

hence $\|\phi(x)\|_2 = \|x\|_\phi \leq \|x\|_2$. Finally, we use the fact that $\|z\|_2 \leq \|z\|_1$ for every $z \in \mathbb{R}^D$ to show the last inequality. We define $z \in \mathbb{R}^D$ such that

$$\forall k \in \llbracket 1, D \rrbracket, z_k = \|x_{I_k}\|_\phi,$$

and we have $\|z\|_1 = \sum_{k=1}^D \|x_{I_k}\|_\phi = N_\phi(x)$. Furthermore,

$$\begin{aligned}
\|z\|_2^2 &= \sum_{k=1}^D \|x_{I_k}\|_\phi^2 = \sum_{k=1}^D \langle x_{I_k}, \phi(x_{I_k}) \rangle \\
&= \sum_{k=1}^D \sum_{i \in I_k} [x]_i [\phi(x)]_i = \sum_{j=1}^d [x]_j [\phi(x)]_j \\
&= \langle x, \phi(x) \rangle = \|x\|_\phi^2.
\end{aligned}$$

□

Now, we can prove Theorem 3.4.

Proof. Under the same assumptions as for Theorem 3.3, and with the gradient updates defined in (2), we have

$$x_+ = x - \eta \frac{\phi(\nabla f(x))}{\Gamma(\phi(\nabla f(x)))}.$$

The gradient centralization operator is linear, self-adjoint and such that $\phi^2 = \phi$. We note $\|\cdot\|_\phi^2 = \langle \cdot, \phi(\cdot) \rangle_2$ the pseudo-norm induced by ϕ . Using (13) with the iterates of (2) gives us

$$\begin{aligned}
F(x_+) &\leq F(x) - \eta \left\langle \nabla F(x), \frac{(\phi \circ \nabla f)(x)}{(\Gamma \circ \phi \circ \nabla f)(x)} \right\rangle + \eta^2 \frac{L}{2} \left\| \frac{(\phi \circ \nabla f)(x)}{(\Gamma \circ \phi \circ \nabla f)(x)} \right\| \\
&\leq F(x) - \eta \left\langle \nabla F(x) - \nabla f(x), \frac{(\phi \circ \nabla f)(x)}{(\Gamma \circ \phi \circ \nabla f)(x)} \right\rangle - \eta \left\langle \nabla f(x), \frac{(\phi \circ \nabla f)(x)}{(\Gamma \circ \phi \circ \nabla f)(x)} \right\rangle + \frac{\eta^2 LD}{2} \\
&\leq F(x) - \eta \sqrt{D} \|\nabla F(x) - \nabla f(x)\|_2 - \eta N_\phi(\nabla f(x)) + \frac{\eta^2 LD}{2}, \tag{20}
\end{aligned}$$

where the last inequality comes from Lemma A.3 and the first part of Lemma A.4. We can derive the following upper-bound using the second and third parts of Lemma A.4:

$$\begin{aligned}
\|\nabla F(x)\|_\phi &\leq \|\nabla F(x) - \nabla f(x)\|_\phi + \|\nabla f(x)\|_\phi \\
&\leq \|\nabla F(x) - \nabla f(x)\|_2 + N_\phi(\nabla f(x)). \tag{21}
\end{aligned}$$

Finally, we use (20) to upper-bound $N_\phi(\nabla f(x))$ and inject it in (21) to get

$$\|\nabla F(x)\|_\phi \leq \frac{F(x) - F(x_+)}{\eta} + (1 + \sqrt{D}) \|\nabla F(x) - \nabla f(x)\|_2 + \frac{\eta LD}{2}. \tag{22}$$

We can conclude the proof using the same argument as for Theorem 3.3. □

Theorem 3.1 (Escaping from narrow local minima). Let x_t be the sequence of iterates defined by (2) and y_t the sequence of iterates of gradient descent,

$$y_{t+1} = y_t - \eta_{\text{GD}} \nabla F(y_t). \quad (4)$$

Assume that $x_t \in \mathcal{B}(x^*)$ (resp. $y_t \in \mathcal{B}(x^*)$) i.e. the ball contained in the basin of attraction of x^* , defined in Definition 3.1. Also, assume that x_t (resp. y_t) is not a critical point i.e. $\nabla F(x_t) \neq 0$ (resp. $\nabla F(y_t) \neq 0$). If the stepsize is sufficiently large,

$$\eta_{\text{SING}} \geq \frac{2r}{\sqrt{D}}, \quad \eta_{\text{GD}} \geq \frac{2r}{\|\nabla F(y_t)\|_2}, \quad (5)$$

then the iterates x_{t+1} (resp. y_{t+1}) is outside the set $\mathcal{B}(x^*)$. See Figure 1 for an illustration.

Proof. Let us consider the more general setting

$$x_{t+1} = x_t - \eta g_t. \quad (23)$$

Provided $g_t \neq 0$, we can note $\|x_{t+1} - x^*\|_2^2$ is a degree two polynomial in η :

$$\|x_{t+1} - x^*\|_2^2 = \|g_t\|_2^2 \left(\eta - \left\langle \frac{g_t}{\|g_t\|_2^2}, x_t - x^* \right\rangle \right)^2 + \|x_t - x^*\|_2^2 - \left\langle \frac{g_t}{\|g_t\|_2^2}, x_t - x^* \right\rangle^2. \quad (24)$$

Cauchy-Schwartz inequality ensure the term outside the square is always positive. Hence

$$\|x_{t+1} - x^*\|_2 \geq \|g_t\|_2 \left| \eta - \left\langle \frac{g_t}{\|g_t\|_2^2}, x_t - x^* \right\rangle \right|. \quad (25)$$

Therefore, for $\eta \geq \left\langle \frac{g_t}{\|g_t\|_2^2}, x_t - x^* \right\rangle + \frac{r}{\|g_t\|_2}$ we have that if $x_t \in A(x^*) \setminus \{x^*\}$, $x_{t+1} \notin A(x^*)$. In the worst case, the RHS is equal to $2r/\|g_t\|_2$. We can further simplify this bound by considering the expression of g_t :

$$g_t^{\text{GD}} = \nabla F(x_t), \quad \|g_t^{\text{GD}}\|_2 = \|\nabla F(x_t)\|_2, \quad (26a)$$

$$g_t^{\text{NGD}} = \frac{\nabla F(x_t)}{\|\nabla F(x_t)\|_2}, \quad \|g_t^{\text{NGD}}\|_2 = 1, \quad (26b)$$

$$g_t^{\text{SING}} = \frac{\phi(\nabla F(x_t))}{\Gamma(\phi(\nabla F(x_t)))}, \quad \|g_t^{\text{SING}}\|_2 = \sqrt{D}, \quad (26c)$$

where NGD stands for normalized gradient descent. Therefore, to ensure $x_{t+1} \notin A(x^*)$ it is sufficient to have

$$\eta_{\text{GD}} \geq \frac{2r}{\|\nabla F(x_t)\|_2}, \quad (27a)$$

$$\eta_{\text{NGD}} \geq 2r, \quad (27b)$$

$$\eta_{\text{SING}} \geq \frac{2r}{\sqrt{D}}. \quad (27c)$$

□

B Additional experiments

B.1 Comparison against other optimizers

We compared other optimizers on the RDE dataset for depth estimation (Section 5.2). We chose this dataset to make the comparison because training a ViT-S on this task using Adam is unstable, and most competing methods try to fix Adam’s instabilities. For all the optimizers, we carefully tuned the learning rate and weight decay using the same methodology as for the classification task in ImageNet (see Section 5.1). We set other hyper-parameters to their default value. The results are available in Table 5. Notably, we found that most optimizers simply do not converge: the combination of AdamW and SING sometimes outperform competitors by a factor of **100** in terms of test loss. Notably, most of the competitors do not use decoupled weight decay [28]. We claim this is part of the reason why AdamW, AdaBelief and AdaFactor (which include it by default) outperform their counterparts by a factor of ten.

	Learning rate	Weight decay	Test loss ($\times 10^{-3}$)	Accuracy
AdamW + SING	5×10^{-2}	5×10^{-2}	0.34	96.56%
Lamb [53]	1×10^{-2}	5×10^{-4}	0.50	93.50%
NAdam [15]	1×10^{-3}	5×10^{-5}	28.3	0.02%
Yogi [55]	1×10^{-2}	5×10^{-5}	24.3	0.24%
AdamW [23, 28]	1×10^{-3}	5×10^{-2}	1.70	78.13%
AdaBelief [60]	1×10^{-3}	5×10^{-4}	3.73	60.26%
AdaFactor [39]	1×10^{-2}	5×10^{-4}	1.87	74.98%
RAdam [26]	1×10^{-3}	5×10^{-5}	20.1	0.75%
AdaBound [29]	1×10^{-3}	5×10^{-5}	38.2	0.03%

Table 5: List of the performance and best-performing hyper-parameters for the training of a ViT-S on RDE using different optimizers. As suggested by the ablation study, normalization is the main reason why SING works but doesn’t fully explain its success.

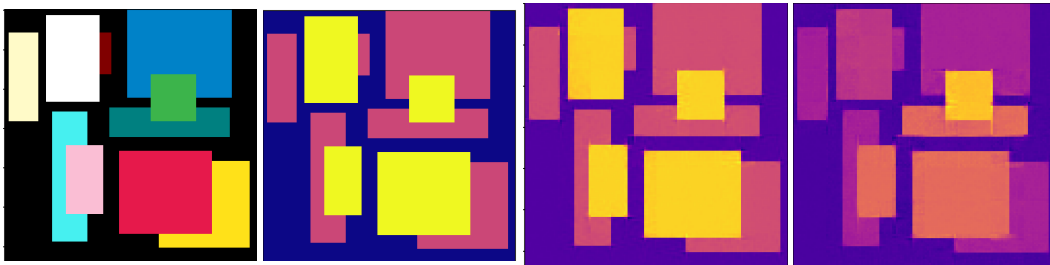


Figure 5: Example of predictions on the RDE [8] dataset. From left to right: input to the network, associated ground truth, prediction using AdamW + SING, prediction using AdamW. The mean squared error for AdamW + SING is 3×10^{-4} and 5×10^{-2} for AdamW.

C Training details

C.1 Depth Estimation

The metric we used to measure accuracy consists in averaging the prediction given for each visible pixel of each rectangle. Then a prediction counts as 1 if *every* rectangle within the image was attributed a correct depth. Examples of images of the dataset can be seen in Figure 5, as well as predictions when trained with AdamW and AdamW+SING. Each training lasts for one hour and a half on one Tesla V100 GPU with 32GB of VRAM.

For the evaluation of SING when combined with other optimizers, we carefully tuned each method using the same method as for ImageNet. We then reported the result corresponding to the best test loss. All the hyper-parameters can be found in Table 6. In particular, while training AdaFactor [39] we disabled the option to train with Adaptive Step Size (see [39]) as we found it to lower the performance with and without SING.

To use a ViT for an image-to-image task, we simply got rid of the classification token and instead reverted the patchification of the input: each output token is used to output a patch of the output image. This can create discontinuities on the image at the patch borders, but for the piece-wise constant images of the RDE dataset we didn’t find this to be an issue.

C.2 Classification

As the FFCV library we used had already tuned SGD, we didn’t modify the hyper-parameters. Indeed, when we tried other configurations the performance dropped. For AdamW + GC and AdaBelief, we kept the same hyper-parameters than those found for AdamW. We tested other configurations but found them to be sub-optimal. The best hyper-parameters found for each network are reported in Table 7. Notably, we found as a rule of thumb that the best learning rate of SING was ten times the

	w/ softplus [42]	Learning rate	Weight decay	Accuracy
SGD	N/A	5×10^{-1}	5×10^{-5}	0.02%
SGD + SING	N/A	5×10^{-1}	5×10^{-3}	94.25%
AdamW	×	1×10^{-3}	5×10^{-2}	78.13%
AdamW + SING	✓	5×10^{-2}	5×10^{-2}	96.56%
AdamW + SING	×	5×10^{-3}	5×10^{-2}	89.38%
AdaBelief	×	1×10^{-3}	5×10^{-4}	60.26%
AdaBelief + SING	✓	5×10^{-2}	5×10^{-2}	96.70%
AdaBelief + SING	×	1×10^{-3}	5×10^{-1}	94.31%
AdaFactor	×	1×10^{-2}	5×10^{-4}	74.98%
AdaFactor + SING	✓	1×10^{-2}	5×10^{-2}	73.06%
AdaFactor + SING	×	1×10^{-2}	5×10^{-4}	76.26%

Table 6: List of the best hyper-parameters for the training of a ViT-S on RDE using different combinations of optimizers and SING. N/A stands for Not Applicable.

		Learning rate	Weight decay
ResNet18	SGD	5×10^{-1}	5×10^{-5}
ResNet18	AdamW	10^{-2}	5×10^{-2}
ResNet18	AdamW + SING	10^{-1}	5×10^{-3}
ResNet34	SGD	5×10^{-1}	5×10^{-5}
ResNet34	AdamW	10^{-2}	5×10^{-2}
ResNet34	AdamW + SING	10^{-1}	5×10^{-3}

Table 7: For each configuration, the list of the best hyper-parameters when training on ImageNet.

best for AdamW, and the weight decay to be ten times lower. For AdamW and SING, no weight decay was applied to the biases of the network and to the normalization layers.

For CIFAR100, the training was very cumbersome due to the large tendency to overfitting. We used label smoothing [40] with a value of 0.1 and small batch sizes of 128 to increase the variance. The best learning rate found was also 10^{-1} but the best weight decay was 5×10^{-2} , probably due to the large chance of overfitting. For AdamW, the best learning rate was 10^{-3} and the best weight decay was 5×10^{-1} . We also froze the learning of the batch normalization’s parameters. We carefully verified that these choices benefited all optimizers. The data were augmented using random crops, random horizontal flips and random rotations of maximum 15 degrees. We tuned the hyper-parameters the same way we did for ImageNet. Notably, the optimal weight decay we found for AdamW was 5×10^{-1} and 5×10^{-2} for AdamW+SING.

C.3 Natural language processing

For the training on IWSLT14, we used the code of [50] which is a fork of the FAIRSEQ [33] library. As stated, we took the code as is and launched it but found the BLUE score to be one point lower than the reported one (for AdamW and AdaHessian [50]). We therefore re-tuned AdamW but found the hyper-parameters reported in [48] to be the best. During training, we found the LayerNorm [2] to be the cause of an increasing gradient norm throughout training. We therefore froze the layers and recovered a normal dynamic. Notably, we found our optimizer to generalize better than AdamW, see Figure 6 for more details. For SING, the best learning rate found was 10^{-2} and the best weight decay was 5×10^{-2} . The learning rate is decreased using a cosine decay. For AdamW and for the rest of the hyper-parameters, we copied the setting of [48]: a dropout of 0.3, a cross-entropy loss with Label Smoothing [40] of 0.1, the gradient is accumulated for four iterations, the maximum number of tokens is 4096, the beam size is five and the length penalization is one. The networks are trained for 200 epochs. Notably, the learning rate of AdamW is decayed using an invert square-root scheduler. We tested using a cosine decay but it lowered the final performance.

	SGD	W + SING	AdamW
ResNet18	75.63%	78.24% ($\pm 0.21\%$)	77.95% ($\pm 0.15\%$)

Table 8: Top-1 accuracy on CIFAR100. The results are averaged across five runs and the values are reported in the format mean \pm std.

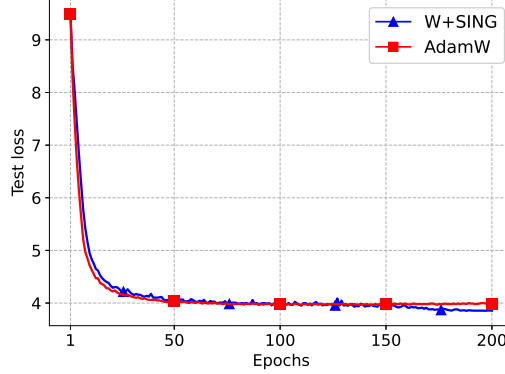


Figure 6: Test losses on the IWSLT14 dataset. We see that the combination of AdamW + SING outperforms AdamW at the end of the training. For AdamW, an inverse square-root scheduling is used as we found it performed best. For AdamW + SING, we used a cosine decay. Overall, it seems SING generalizes better than its counterpart.

For the fine-tuning tasks, we used the code provided by the HuggingFace library as is and launched the trainings, only to find the performance to be lower than suggested. We suspect the numerous changes in the library since the scripts were made to be the cause of it. We trained SING by freezing the LayerNorm layers and tuned the hyper-parameters. For SQuAD, we found the performance to be reached in three epochs instead of just two for AdamW. This suggests SING overfits less rapidly than AdamW. Since the trainings were very fast, we could afford to tune more our hyper-parameters: the best learning rate found was 8×10^{-4} and the weight decay 3×10^{-3} . For AdamW, it was 3×10^{-5} and 0. For both optimizers, the best batch size was 12. For SWAG, the best batch size is 32, the number of epochs is four, the best learning rate is 2×10^{-4} and the best weight decay is 3×10^{-3} .

C.4 On the learning rate scheduler

Theorem 3.1 suggests that the learning rate must be as high as possible to escape narrow local minima. Therefore, it would make sense to consider a learning rate scheduling that keeps the learning rate constant to a high value for as long as possible. Then, once all the narrow local minima have been escaped and a large one has been found, the learning rate can be decreased to converge. While this strategy works, we found in practice that using a cosine decay to be working slightly better. We argue this strategy is to be preferred as it doesn’t involve any tuning.

D Other properties

D.1 Invariant to gradient clipping

The update given by (2) cancels most clipping strategies. Indeed, most clipping strategies amount to multiplying the gradient by a certain factor (for instance $\alpha/\|\nabla f(x)\|_2$ or $\alpha\|x\|_2/\|\nabla f(x)\|_2$). Since ϕ and Γ are both homogeneous operators, the normalization cancels any layer-wise multiplication of the gradient by a scalar.

E Broader impact

The goal of our technique is to improve the stability of the training of neural networks. This may open the door to further improvements in neural networks as the architecture of tomorrow might be difficult to train with the today's optimizers. Our technique also allows for faster trainings, which reduces the amount of energy needed to train one network. Furthermore, our method allows the usage of light hyper-parameter-search strategies which further reduces the need in resources.

There are risks associated with easier and better training of neural networks, as these aspects will also benefit applications that can be detrimental to society. In addition, better learning on a biased dataset might result in networks with stronger biases (e.g. [4]). While such biases are considered to be caused by the dataset, they could be exacerbated by the model capacity and the effectiveness of the training algorithm.